*Arab J. Nucl. Sci. Appl., Vol. 58, 1, 43-55 (2025)*

ISSN 1110-0451

***Arab Journal of Nuclear Sciences and Applications***

***Web site: ajnsa.journals.ekb.eg***

(E S N S A)

# Study of Thermal and Mechanical Effects on Materials during Heat Transfer in Supercritical Regime

**Samaa A.Wasfy, Magy M. Kandil, Ahmed M. Refaey and Salwa H. Abdel-Latif**

*Nuclear & Radiological Safety Research Center, Egyptian Atomic Energy Authority (EAEA), Cairo, Egypt.*

ARTICLE INFO

*Article history:*

Received: 20th Aug. 2024

Accepted:13th Oct. 2024

Available online: 1st Nov. 2024

*Keywords:*

*SCWR;*
*heat transfer coefficient;*
*mechanical analysis;*
*ANSYS code.*

ABSTRACT

**Heat transfer and material design are two vital technology areas in the development and licensing of Super Critical Water Reactors (SCWR). It has a direct impact on safety criteria that are based on peak cladding and fuel centerline temperatures. A high cladding temperature leads to high thermal stresses on the material, so the stress and strain across the pipe wall thickness were calculated. Cladding temperature is evaluated using heat transfer correlations. In the current work, the heat transfer coefficient of the supercritical pressure mode of water in a vertical-upward circle pipe was investigated numerically. Thermal-hydraulics and static structural modules of the ANSYS code were used to create a model that can be used for calculations. The FLUENT module calculates the thermal-hydraulic parameters as surface and water temperatures in the axial direction, while the static structural module is used to calculate the stress and strain fields across the wall surface. The prediction model's results are contrasted to measurements from the famous Watts experiments. These experiments were carried out in a uniformly heated tube to examine the effect of high pressure and temperature on water's heat transfer behavior. In this paper, new correlations of heat transfer coefficients were predicted by the created model. These correlations were evaluated for accuracy by comparing them with the other correlations.**

## 1. INTRODUCTION

Effective transfer of heat from heated walls to fluids is a critical topic in industry. The point of critical heat flux is a thermal condition that reduces heat transfer rate. As soon as the heat flux of the heated wall reaches a certain threshold, the fluid becomes incapable of effectively removing the heat from the wall, and the temperature of the heated wall increases sharply, causing burning and wall damage.

The coefficient of heat transfer is a crucial factor in the design of SCWR. At the supercritical stage, there are three types of heat transmission: usual, enhanced, and waned. The heat transmit response of supercritical water in the pseudo-critical range differs from that of single-phase fluids in the sub-critical range.

The most important goals of using high-pressure water conditions in nuclear power plants are to increase NPP productivity, reduce capital and operating costs, and lower electrical energy costs [1&2]. This would improve the sustainability of nuclear power by reducing fuel consumption for power generation, resulting in less spent fuel for disposal. Furthermore, the safety characteristics of SCWR have improved with the introduction of passive safety systems. Depending on the concept configuration, expansion resistance and protection against harm are improved.

Experimental studies at supercritical water conditions were implemented in circular tubes [3–6], theoretical researches have mostly concentrated on the heat transfer to supercritical water using experimental measurements at normal conditions. More than thirty correlations describing the heat transfer coefficient (HTC) and above ten criteria predicting the start of DHT are established in the literature. A thorough review of the different correlations is presented for example in [7–10]. In order to find the greatest suitable correlations, several studies have evaluated the various correlations and criteria.

Corresponding author: samaaahmedwasfy1812@yahoo.com

DOI: 10.21608/ajnsa.2024.314013.1842

Stress, corrosion, and cracking are major concerns throughout the core. The present awareness of how to react candidate materials to SCWR systems was reviewed, with a focus on corrosion and stress corrosion cracking responses, as well as the design-trade-offs supplementary with specific alloy-systems. Ferritic-martensitic steels have great resistance to stress-corrosion-cracking, but maximum severe oxidation.

Nickel alloys and stainless steels are more resistance to oxidation, however, they are additional prone to stress weathering cracking [11] .Hoop stress due to pressure inside is a main stress that determines the rest life of the tube in the conventional fuel power plant's repeater. However, thermal stress caused by temperature differences through the pipe wall diminished the tube's life.

As a result, thermal loads must be considered, despite the fact that internal pressure loading has been shown to contribute significantly more to tube stress than thermal loads.

The impact of the heat transfer coefficient on thermal stress was studied before. The Studied found, the heat transfer coefficient at the outer surface has a greater effect on the thermal stress than at the inner surface. Also, when thermal loading was considered without internal pressure loading, the hoop stress was greater than the radial stress for both uniformly thinned and eccentrically thinned tubes [12].

## 2. WATTS EXPERIMENT (1980):

Data for supercritical water from the famous experiments 'Watts' were accompanied in an equally heated tube with an outer diameter of 2.54 cm and a length of 200 cm. An unheated length of 78 cm was in the entrance of the tube. The experiments boundary conditions are 250 bar pressure, 175 to 400 KW/m2 as the heat flux and the inlet temperature values (150, 200, 250, and 300 C), and inlet mass fluxes ranging from 200 to 1000 kg/m$^2$ s. A natural circulation loop was used to produce the flow, and the test section was heated electrically. The inside tube temperatures were inferred by the measurement of the outside surface values.

During normal SCWR operation, the coolant remains a single-phase fluid. So, the ordinary safety margin of critical heat flux for nuclear power plants is no longer relevant. Nevertheless, pressure decreases in loss of coolant accident scenarios and SCWR shutdowns, while pressure increases during SCWR startup. These pressure changes may cause critical heat flux in the fuel assemblies, resulting in a shrill increase in clad fuel temperature and recommending to the cladding's safety.

## 3.COMPUTATIONAL FLUID DYNAMICS (CFD) TOOL

CFD is a common method for analyzing complicated flow and heat in manufacturing issues. In this article, the thermal fluid parameters in heat convection are studied using the capabilities of the ANSYS FLUENT 17.2 [13] program. Various mesh solutions and models for turbulence were used to address water flow issues such as temperature.

### 3.1. Description of the ANYSIS Model

In order to create the supercritical water transfer of heat approach, the equations that govern it were determined using the technique of finite volumes. The Fluent code is implemented for computational modeling. The numerical simulation exactly mirrors the Watts experiment. The model consists of its testing section, which is the examine pipe shown in figure (1) at a constant pressure of 250 bar. The pipe wall is assumed to have uniform heat flux. The heating flux is directed to the heated wall material. The liquid stage's characteristics can vary according to the operating conditions. Table 1 lists the controlling parameters for the numerical model. The theoretical predictions are validated with the experimental measurements.

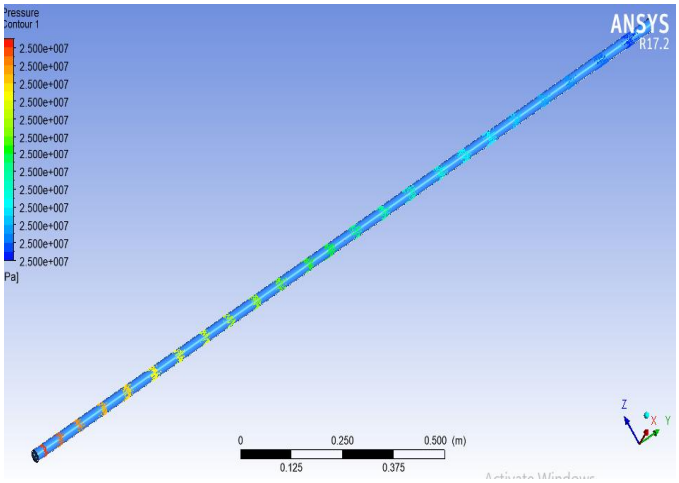


**Fig. (1): ANSYS Model (Test Pipe)**

**Table 1**

| Item | Value |
|---|---|
| pressure (MPa) | 25 |
| Heat flux (Kw/m2) | 250, 340,400 |
| Mass Flux (Kg/m2.s) | 318,345,392,410 |
| Inlet temperatures (oC) | 150, 200,250 |

### 3.2. Numerical Solvers of the FLUENT Module

The used module lets you select one from two solvers: a pressure-based solver and a density-based solver, in both methods, the velocity field is obtained from the momentum equations. The SIMPLE scheme is used in the current study for pressure velocity coupling, and simulations were carried out using the pressure-based solver Fluent 17.2 with buoyancy effects included in into account.

### 3.3 The model approach and assumptions.

As mention above, the pressure-based approach was used, in this Solver approach, the pressure field is extracted by solving a pressure or pressure correction equation which is obtained by manipulating the continuity and momentum equations. Using either method, The ANSYS FLUENT17.2 will solve the governing integral equations for the conservation of mass and momentum, and, when appropriate, for energy and other scalars such as turbulence. Turbulent flow is assumed for all runs, leading to **the Reynolds-Averaged Navier–Stokes equations (RANS),** which were then discretized by the finite volume method. The turbulence model used for enclosed domain was the **κ–ε** standard approach and **κ–ω SST** approach.

With the results verification, the **κ–ω SST** approach is suitable for the experimental model.

### 3.4. The Geometry and mesh of the model

The FLUENT model of the test pipe involves the entire axially measurement of 2 meters. The actual geometrical size of the test pipe and the mesh size were used. Small geometric details were modeled. The computation mesh within the structure was created using hexahedral computation nodes, and the resulting mesh resolution is shown in Table 2 and Figure 2.

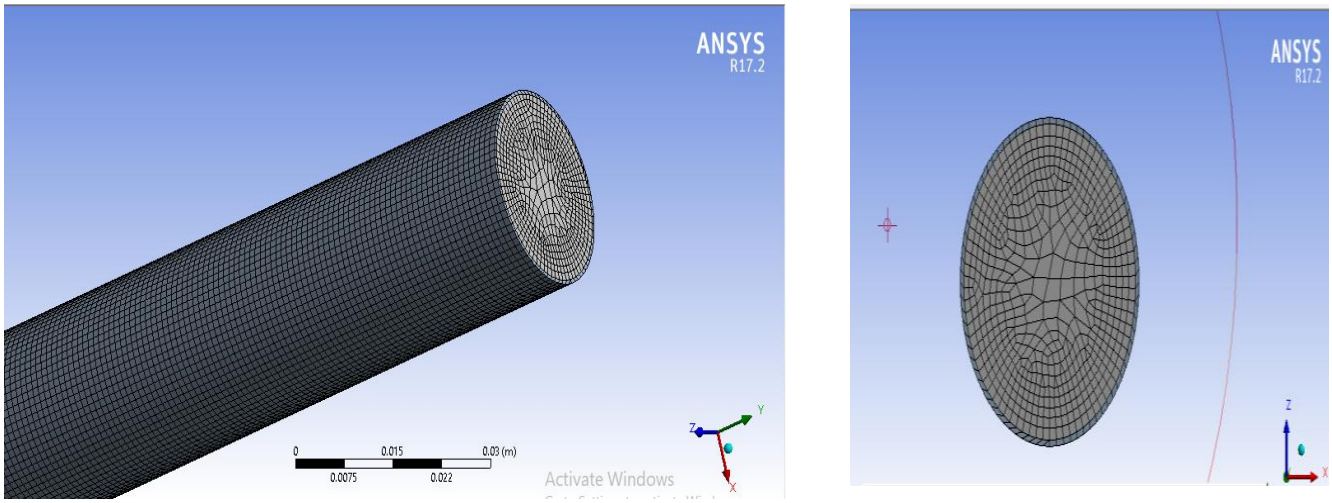


**Fig. (2): The FLUENT model of the Test pipe and its mesh**

**Table (2)**

| Details of "Mesh" | |
|---|---|
| Nodes | 1402000 |
| Elements | 1343328 |
| Mesh Metric | Skewness |
| Min | 1.7417e-002 |
| Max | 0.74314 |
| Average | 0.17197 |
| Standard Deviation | 0.16542 |

**The mesh resolution as shown in table 2 is in line with ANSYS best practice guidelines for modeling forced convection flows as shown in Fig. (2).**

### 3.5. Model Validation

The thermal hydraulic FLUENT model was validated by comparing the calculated wall temperatures with experimental measurements. The experimental measurements for the case of 25 MPa pressure, 250 kW/m2 uniform heat flux, 200°C inlet temperature, and two distinct mass fluxes of 318 and 356 kg/m2 are presented.

Figure (3) shows the agreement between the calculated surface temperatures and those obtained from literature measurements. The validated model is using to calculate the effect of various parameters on surface temperature, including heat flux, mass flux, and inlet temperature.

The current model shows a weakened coefficient of heat transmission deterioration, the same as that observed at higher mass fluxes, as temperatures that were greater were experimentally measured. As a result, the suggested model appears to predict a narrower and earlier change area; however, improvements are observed when the mass flux is reduced by a small amount, such as 3%. Watts (1980) stated that mass flow measurements have an accuracy of ±3%, making the proposed condition reasonable.

## 4. RESULTS AND DISCUSSION

In this part of the article, the relationship between the several runs carried out to investigate the surface temperature at various mass fluxes, heat flux, and inlet temperature of water is discussed.

### 4.1. Effect of mass flux (G) Kg/m$^2$.s

The distribution of the wall surface temperature at heat flux 250 kW/m2 on the pipe surface is scanned. Figure (4) shows how the surface temperature varies with axial distance along the test pipe. The temperature rises as the length of the pipe increases. In the case of G = 318 Kg/m2.s, the wall temperature increases from the start at the first section, where Z/D = 4, to reach 343 $^{o}$C at the third section, where Z/D = 17. Also, we can see the same temperature behavior distribution in all cases of mass flux values.

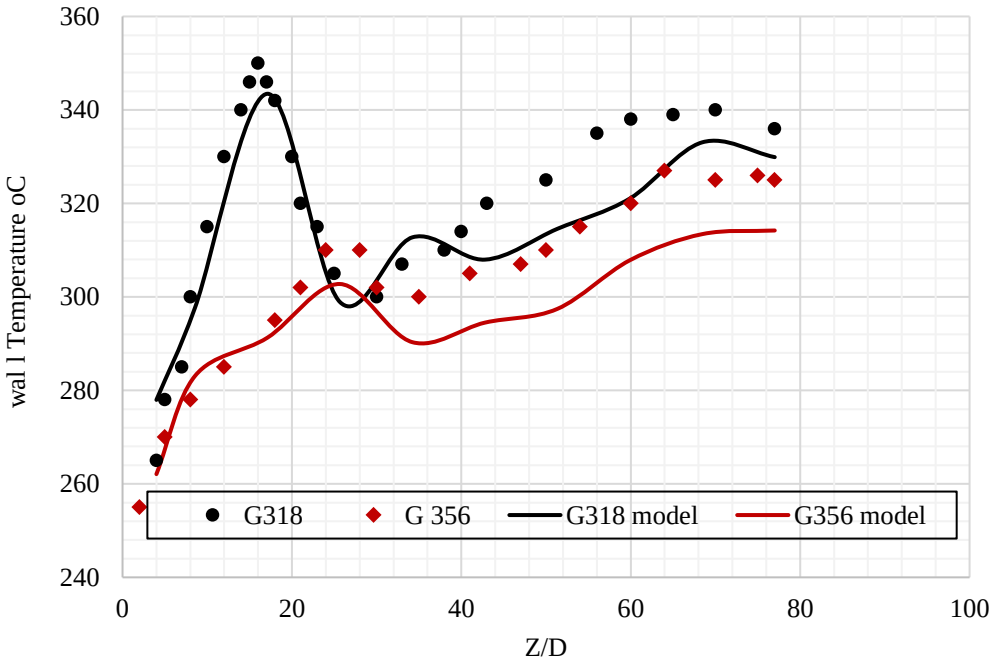


**Fig. (3): Comparison between the calculated and measurement wall surface temperatures with different mass flux for upward flow**

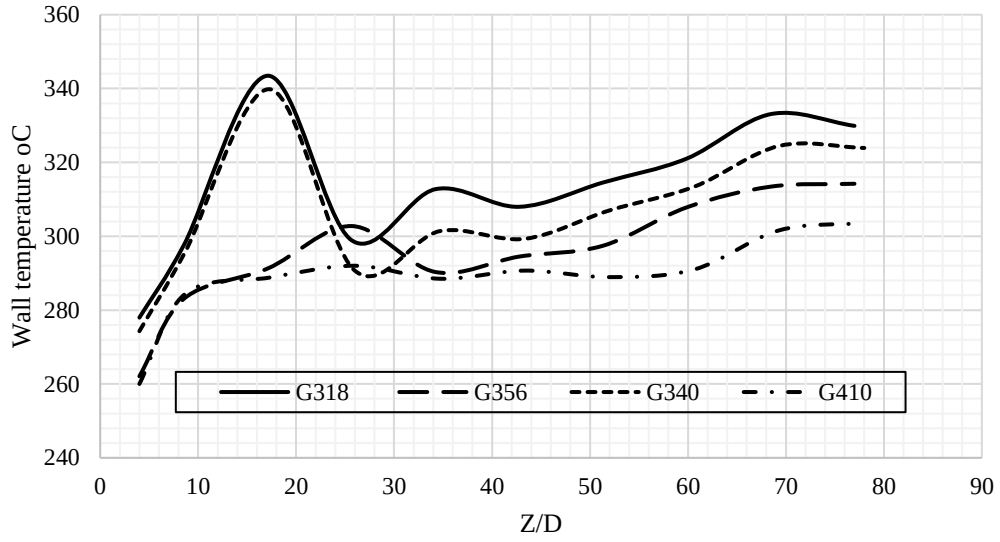


**Fig. (4): the variation of axial wall surface temperature with different G At 200 ºC and 250 W/m$^2$**

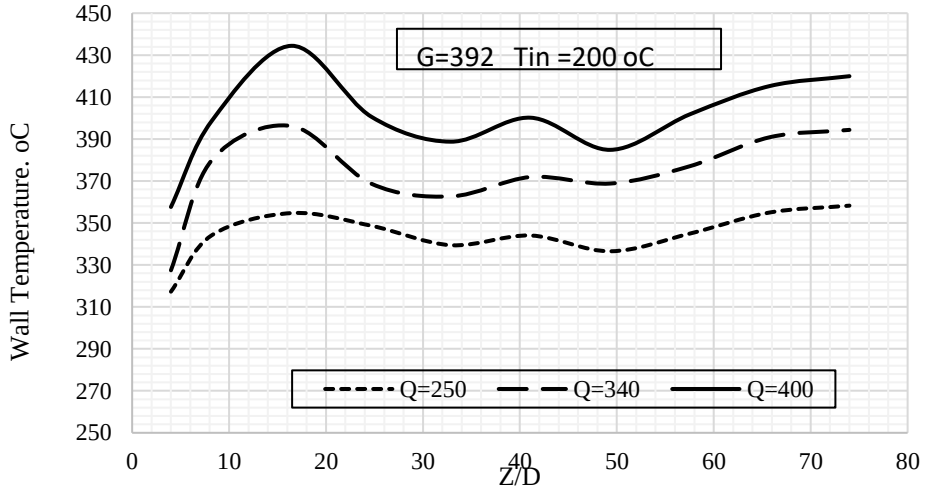


**Fig. (5): Variation of axial wall surface temperature with different Q at $T_{in}$ =200 ºC and G =392 Kg/m$^2$.s**

The measured wall temperature trend completely changes when moving from G = 340 kg/m2. S to G = 356 kg/m2. S, which represents a relative mass flux increase of approximately 4.7%. This could be due to the increase in fluid velocity. It means that as mass flow increases, so does the heat transfer coefficient.

### 4.2. Effect of heat flux

Initially, a constant heat flux is set up throughout that heated section; greater variations can be observed when the flux increases. No significant differences occur when the flux is reduced. Additional analyses were carried out using a variable heat flux along the heated length. Because direct heating was used in these experiments, the imposed heat flux is highly dependent on the local wall temperature.

Figure (5) displays the surface temperature behaviour during varying the heat flux from 250 to 400 W/m$^2$ at constant inlet temperature (200 oC). The surface wall temperature decreases with decreasing the heat flux; this is due to the rise in temperature difference. In this case, the practical heat transfer deterioration phenomena are probably due to a combination of flow acceleration and surface temperature more than the pseudo-critical point.

### 4.3. Effect of inlet temperature

The variant of the wall surface temperature along the pipe with various inlet temperatures is conducted in figure (6). From the figure, the wall temperature increases along the height of the pipe, from the start at Z/D=17, where the temperature exceeds 350 ºC in the case of a 250 ºC inlet temperature to reaching 360 ºC at the last section at Z/D=76 at the same inlet coolant temperature. Moreover, we can get the distribution of temperature increasing with an increase in the inlet temperature of the coolant.

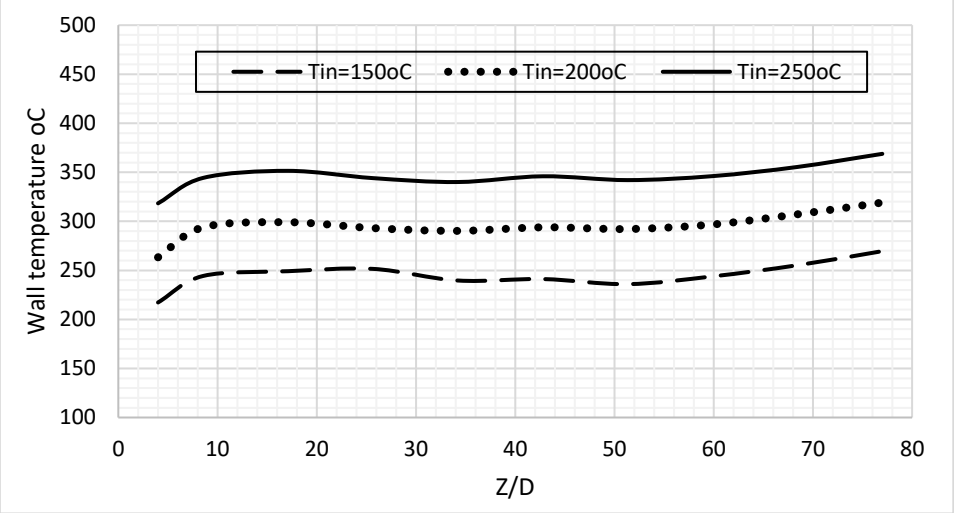


**Fig. (6): Variation of axial wall surface temperature with different Q at $T_{in}$ =200 ºC and G =392 Kg/m$^2$.s**

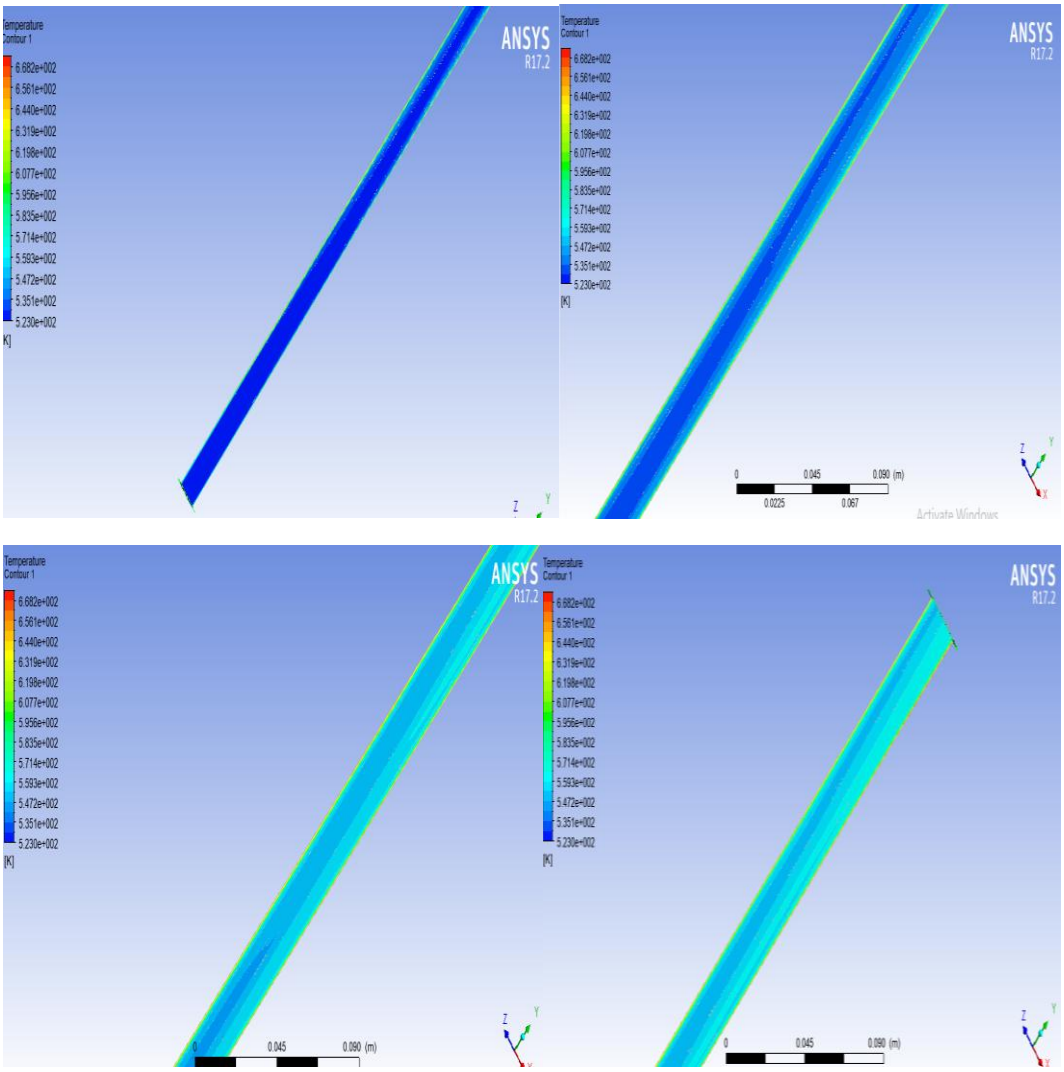


**Fig. (7): the contours of temperature and the variation at four zones values (Z/D=4, 17, 42 and 76) respectively (a, b, c and d)**

From the figure, it is displayed that the surface temperature rises along the height of the pipe. Moreover, there is a decrease in the wall surface temperature in the intermediate layers of the pipe due to improved efficiency of heat transfer.

### 4.4 The visualized Temperature using FLUENT Model

Because the test pipe is so long (Z = 2.0 m), examining the particulars of the entire flow field in the pipe is challenging. With four zones selected, start at (Z/D=4, 17, 42, and 76). The analysis focused on these layers. The results of the FLUENT model are documented. These results are characterized as the visualized temperature.

The variation of the colors represents the wall temperature and the contour showed the high temperatures for the layers previous and next to the most severe zone. The visualized results are congruent with the two-dimensional results shown in figure (7).

The variation of the colors represents the wall temperature distribution. The contour displays the layers with the highest degree of temperatures around the most severe zone. The envisioned results are matching with the 2-D results illustrated in figure 7.

## 5. ASSESSMENT OF THE CORRELATIONS

The Dittus-Boelter equation is a commonly used experimental correlation for involuntary turbulent flow in pipes, which provides a respectable approximation for flows away from the supercritical area. Nevertheless, it has been found that at supercritical pressures the HTC can deviate from this equation significantly, specifically near the pseudo critical temperature (Tpc). There are a range of postulates on involving to the mechanisms which give growth to HTD. Calculating the onset of HTD and its subsequent recovery is critical to the reactor design and safety analysis.

### 5.1 Correlation Development

The fluid properties change significantly between the wall and the bulk flow conditions. Internal flow applications operating near the critical point require heat transfer correlations that account for property variations. the properties of water at pressure and temperature were used to calculated the dimensionless parameters as Re Reynolds number, Pr Prandtl number, Nu Nusselt number, Cpw/Cpb , $(\rho_w/\rho_b)$, $(k_w/k_b)$, $(\eta_w/\eta_b)$ and $(1+(z/D))$ and a new correlation of heat transfer coefficient was deduced.

**Prediction of $Nu_b$**

The numerically predicted Nusselt number was calculated as per Equations (1&2). The fluid bulk and wall temperatures were estimated near the pipe outlet. Additional information on the properties and non-dimensional numbers can be calculated as in Table 3. The Nusselt number by the dimensionless numbers as equation 2.

$$h = Q/(T_w - T_b) \quad \text{---------- (1)}$$

$$Nu_b = (h*D)/k \quad \text{---------- (2)}$$

**Table 3**

| |
|---|
| For 350 >Q>200 kw/m$^2$, $T_{in}$>100 $^o$C, G >300 kg/m$^2$.s |
| $Nu_b = 0.954183(R_e)^{0.4341}(P_r)^{-2.1588}(C_{pw}/C_{pb})^{-0.9109}(\rho_w/\rho_p)^{-6.8892}(k_w/k_p)^{8.1164}(\mu_w/\mu_p)^{-0.0002}\left[1+\frac{z}{D}\right]^{0.0045}$ |
| For Q>350 kw/m$^2$, $T_{in}$>200 $^o$C, G >300 kg/m$^2$.s |
| $Nu_b = 0.9995(R_e)^{0.5174}(P_r)^{3.1391}(C_{pw}/C_{pb})^{-0.1361}(\rho_w/\rho_p)^{-1.6647}(k_w/k_p)^{1.8396}(\mu_w/\mu_p)^{0.408}\left[1+\frac{z}{D}\right]^{0.0021}$ |

### 5.2. The variation of axial (Nub) Nusselt number of the pipe (different inlet temperature)

Figure (8) presents the axial ($Nu_b$) Nusselt number based on bulk temperature along the test pipe, whose 2m length. Nu is indication of the heat transfer coefficient. The pipe, according to the results obtained from the model, can be distributed into four segments. The first segment is from the beginning of the pipe until Z/D = 20, where there is a deterioration in the heat transfer coefficient. It was establish that the heat transfer in the two sections from 60 >Z/D >30 is better than that in the last section of the pipe (the end of the pipe). However, this enhanced phenomenon seems stronger at Z/D =60 in all conditions.

## 6. MECHANICAL ANALYSIS:

Thermal stress and strain affected by stream heat transfer in NPPs pipelines are an active region of investigation. Prior investigation was limited to experimental methods and theoretical analysis techniques. Several researchers start using finite element analysis (FEA) software to investigate conduit thermal stresses as a result of the fast development of processer software. The stress distribution was demonstrate from the calculated temperature in the FLUENT module. The static structure module was employed into the thermal hydraulic and static structure couplings. The Static Structure Module is used to investigate the thermal stress and strain in the pipe during water heat transfer in supercritical pressure regime.

### 6.1 ANSYS Mechanical Analysis:

In a geometric model of the pipe domain using simulation, the output temperature distribution from the ANSYS Fluent module is used as input for the ANSYS Static Structure module. The stress on the pipe at all the inlet temperatures (150, 200 and 250 $^oC$) is measured are ~~conducted~~. The ANSYS structure results (thermal stress and strain) are focusing at maximum temperature.

The pipe is modeled with 3D-structural elements, considering the temperature - dependent material behavior. The model embraces only the remaining (not melted) part of the pipe wall. The meshing is kept likewise the one of the thermal model axi-symmetric. The node positions and the element geometries of the pipe wall correspond exactly to those of the thermal model. Thus, an easy transfer of the temperature loads from the thermal model is possible. The structural analysis uses the temperature history and distribution of the ANSYS thermal model, with temperature dependent material properties, thermal loads and boundary conditions.

### 6.2 The Variation of Axial Stresses on the pipe.

The Von Mises failure theory point toward that a material will fail if the Von Mises stress or equivalent stress of that material under load is equal to or greater than the yield limit. The variation of the axial stress, and strain on the pipe with inlet temperature is shown in figures (9, 10). Thermal stress is a comparable stress value based on distortion energy that determines whether a ductile material will fail (yield or fracture) under a given load condition.

The thermal stress varies along the pipe, from inlet to outlet, that is due to the change of the phase of the fluid from the liquid phase to the vapor phase (super steam) in super critical water reactors, from figure 9, at Tin 150 $^oC$ , the stress value is 655 MPa at the inlet of the pipe reached to 773 MPa at 0.45m, then lowers to 711MPa at 1.33m, and increases again to 809MPa at the end of the pipe, at Tin 200 $^oC$, the stress value started with 821 MPa at the inlet, reached to 934 MPa at 0.45m, then lowers to 901MPa at 1m and increases again to 957MPa at the end of the pipe, and finally at Tin 250 $^oC$, the stress value is 987 MPa at the inlet, and 1111MPa at 0.45m, then lowers to 1051MPa at 1.33m then increases to 1123MPa at the end of the pipe, so, with increasing the inlet temperature to 250$^oC$ , the maximum stress is increasing too.

The strain curves ( figure 10) take the same trend of stress curves, it reached to maximum (0.004158) at the end of the pipe for T=150, and for T=200, rise to 0.00492, and for T=250 the maximum strain is 0.00578, so the stress and strain is increasing with the increasing of the temperature.

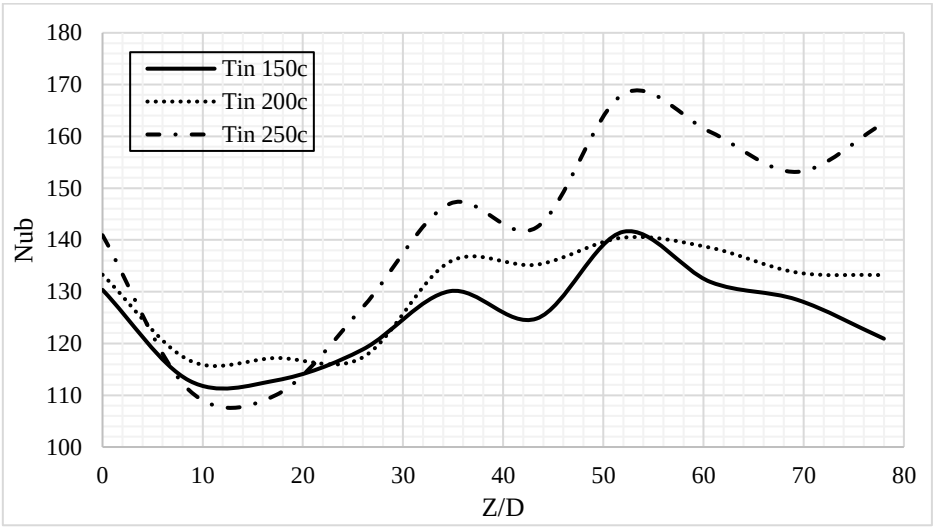


**Fig. (8): The variation of axial (Nu) Nusselt number.**

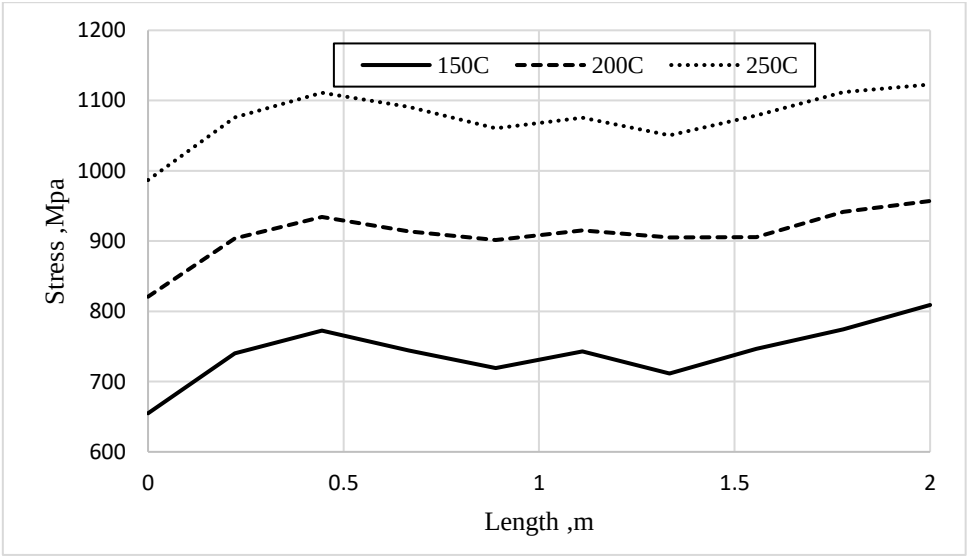


**Fig. (9): The variation of axial thermal stresses on the pipe for steel 304.**

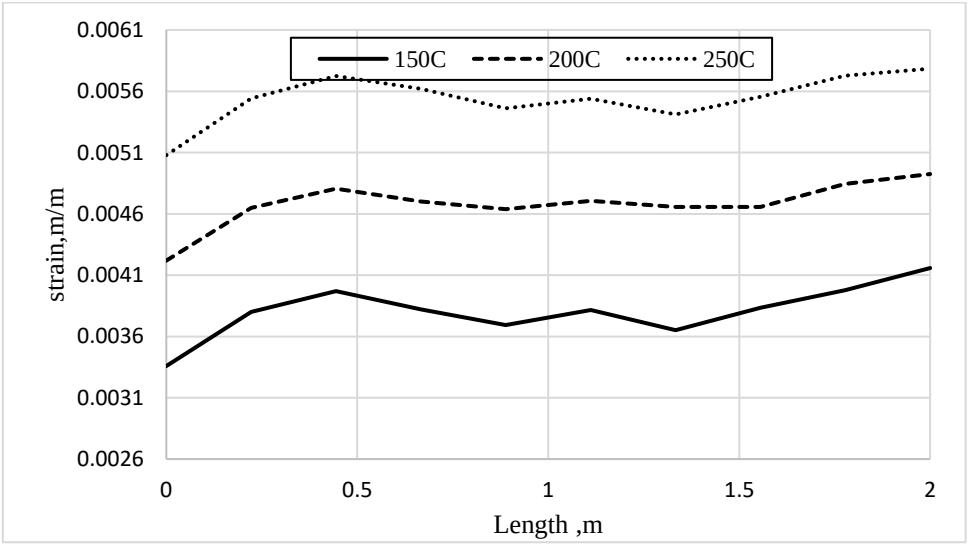


**Fig. (10): The variation of strain on the pipe for steel 304.**

Figures (11, 12, and 13) represent the visualized equivalent Von Mises stress configuration at three positions through the pipe (inlet, middle, and outlet) for the three temperatures used: 150 ºC, 200 ºC, and 300 ºC.

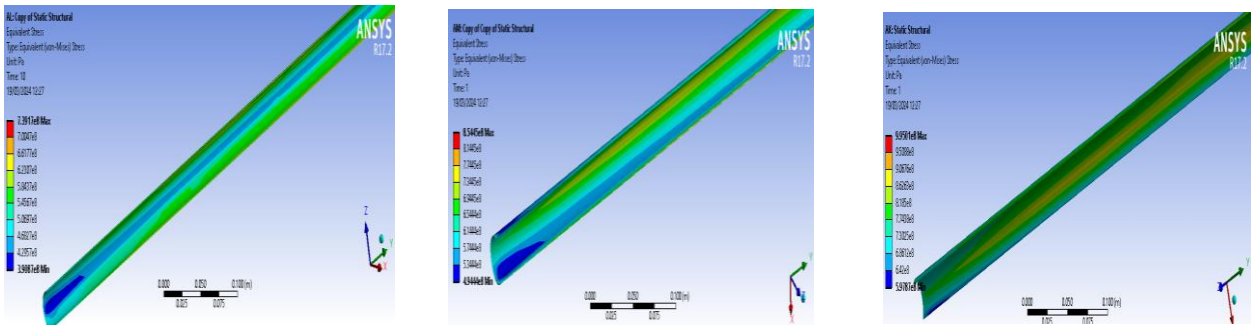

**Fig. (11): Configuration of equivalent stress at the inlet of the pipe at Tin 150,200,250 ºC**

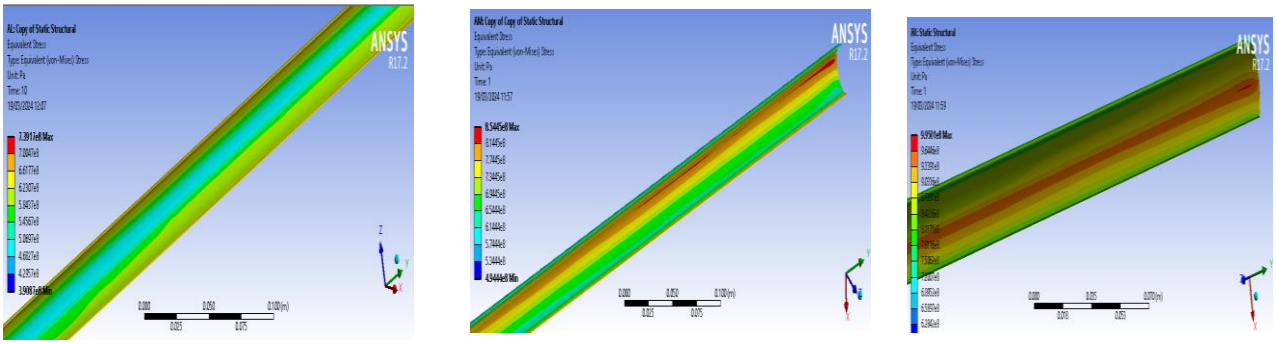

**Fig. (12): Configuration of equivalent stress at the middle of the pipe at $T_{in}$ 150,200,250 ºC**

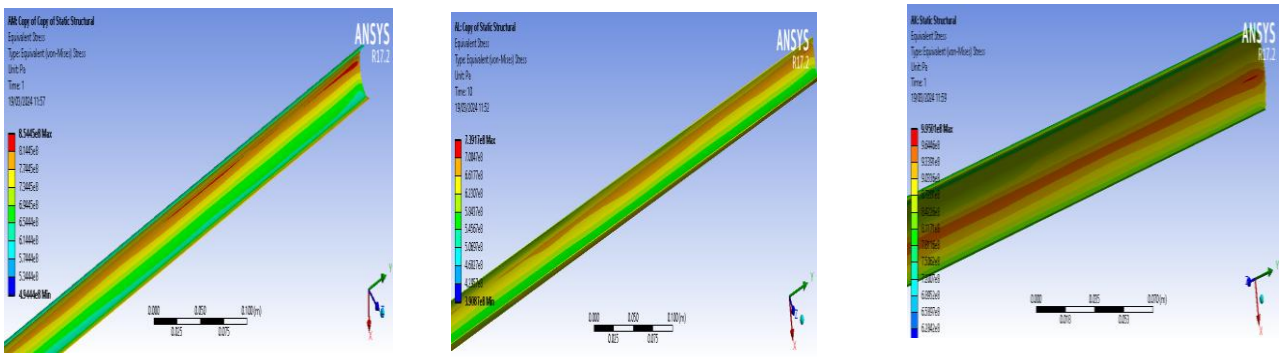

**Fig. (13): Configuration of equivalent stress at the outlet of the pipe at Tin 150,200,250 C**

### 6.3 The effect of Thermal stresses on Different materials at different inlet temperatures

The comparison of the thermal stress of some different materials used in NPP (steel 316L, steel 625, steel 800H, and steel 304L) at different inlet temperatures (150, 200, and 250 °C) is illustrated in figures 14, 15, and 16, respectively. The three figures show the same trend: the stress distribution for st.304 is much closer to st.316 and has the maximum stress, then st.800H, and st.625 has the lower stress. This is due to the fact that the fact that the thermal expansion of st.625 is lower than that of the three other steels, so st.625 has the best mechanical properties to withstand the thermal stresses and strains.

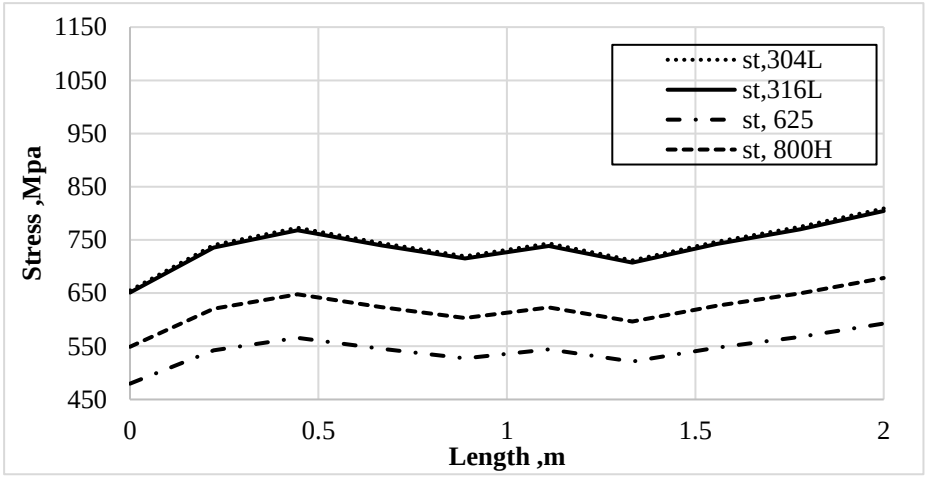


**Fig. (14): the effect of Thermal stresses At $T_{in}$=150 °C**

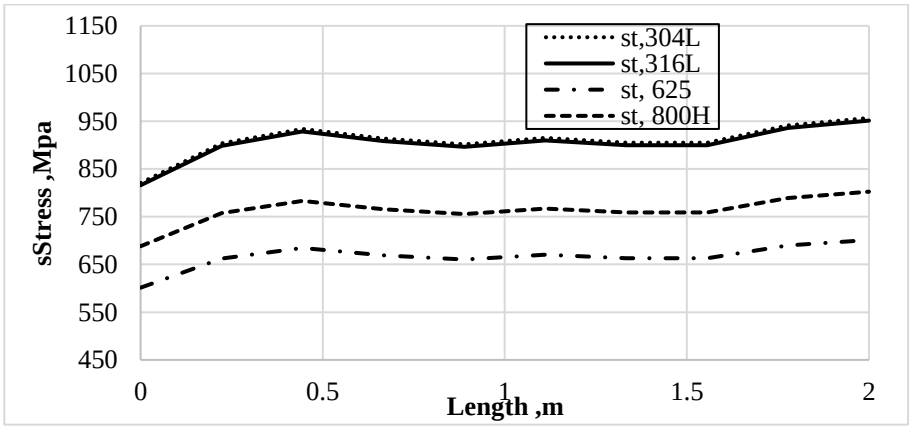


**Fig. (15): the effect of Thermal stresses At $T_{in}$=200°C**

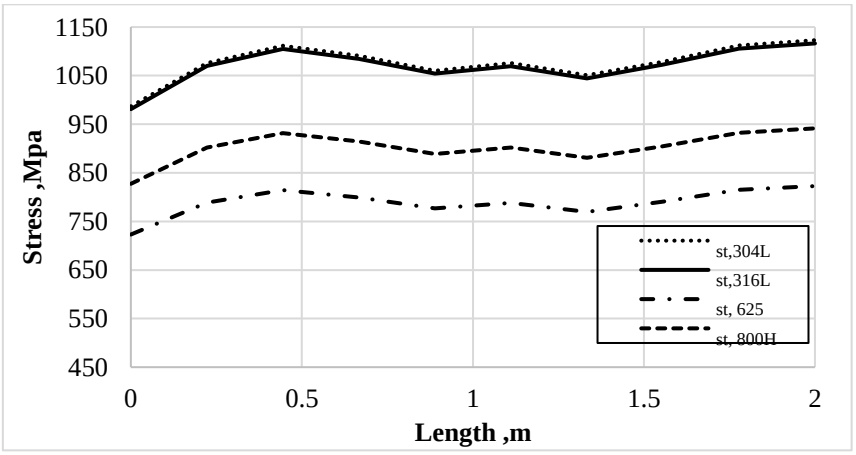


**Fig. (16): the effect of Thermal stresses At Tin=250 °C**

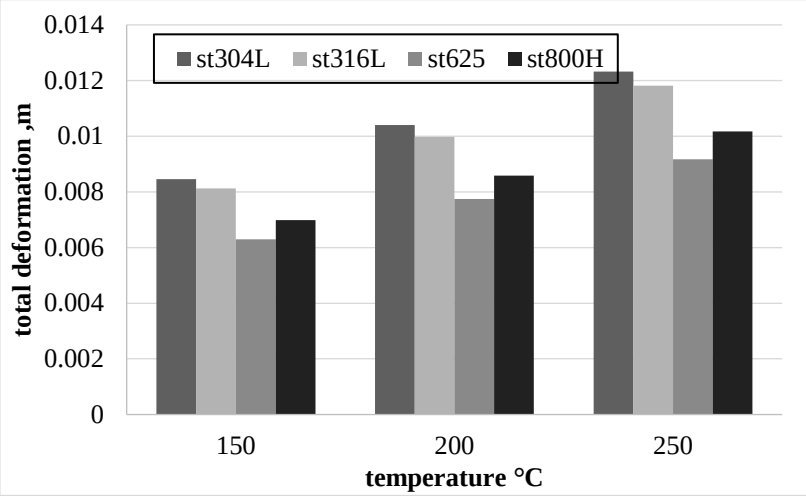


**Fig. (17): total deformation of 4 types of steel with different inlet temperatures**

The comparison between the total deformations caused in 4 types of steel with the different inlet temperatures used is illustrated in Figure (17), from the figure, st.625 has the minimum deformation for all three temperature, then st.800H, and maximum deformation caused in st.316 then st.304.

## 7. CONCLUSIONS

Thermal-hydraulics and structural modules of ANSYS 17.2 are used to create a model that can be used for calculations. Both the axial wall and bulk temperatures from the Fluent 17.2 module are calculated. The numerical predictions are compared to the experimental data from the Watts experiment (1980). The evaluated model was used to find the effect of changing both heat flux, mass flux, and Z/D on the temperatures of the wall and bulk. The properties of water at pressure and temperature were found, and the dimensionless parameters as Re Reynolds number, PrPrandtl number, Nu Nusselt number, Cpw/Cpb , $(\rho_w/\rho_b)$, $(k_w/k_b)$, $(\eta_w/\eta_b)$ and (1+(z/D)) were calculated and a new correlation of heat transfer coefficient was deduced. The stress and strain distribution across the pipe is calculated by the static structural module, at different inlet temperatures. From the results, we got the following: the heat transfer coefficient along the test pipe, whose 2m length is compared. The pipe, according to the results obtained from the model, can be divided into four sections. The first section is from the beginning of the pipe until Z/D = 20, where there is a deterioration in the heat transfer coefficient. It was found that the heat transfer in the two sections from 60 >Z/D >30 is better than that in the end of the pipe. However, this enhanced phenomenon appears to be stronger at Z/D =60 in all limitations. Also it was found that the thermal stress varies along the pipe, from inlet to outlet due to the change of the phase of the fluid from the liquid phase to the super steam phase, the highest stress distribution obtained at T=250ºC, at the end of the pipe, the comparison of some types of steels used in supercritical PPs showed that st.625 gives the best mechanical results. Predicted results demonstrated that this criterion achieves good agreements against the experimental data at various masses, fluxes, and pressures.

## REFERENCE

[1] He, S., Kim, W. S., and Bae, J. H., 2008, “Assessment of Performance ofTurbulence Models in Predicting Supercritical Pressure Heat Transfer in aVertical Tube,” Int. J. Heat Mass Transfer, 51, pp. 4659–4675.

[2] Cheng, X., Kuang, B., and Yang, Y. H., 2007, “Numerical Analysis of HeatTransfer in Supercritical Water Cooled Flow Channels,” Nucl. Eng. Des., 237,pp. 240–252.

[3] Ang, F.; Yang, J.; Gu, H.-Y.; Zhao, M.; Li, H.-B.; Lu, D.-H.: Experimental research on heat transfer performance of supercritical water in vertical tube. YuanzinengKexueJishu/Atomic Energy Science and Technology 47 (2013) 933–939, 10.7538/yzk.2013.47.06.0933

[4] Shen, Z.; Yang, D.; Xie, H.; Nie, X.; Liu,W.; Wang, S.: Flow and heat transfer characteristics of high-pressure water flowing in a vertical upward smooth tube at low mass flux conditions. Applied Thermal Engineering 102 (2016) 391–401, DOI:10.1016/j.applthermaleng.2016.03.150

[5] Mokry, S.; Pioro, I.: Improvement of Supercritical Water Heat- Transfer Correlations for Vertical Bare Tubes. in: Proceedings of the 22nd International Conference on Nuclear En-gineering, Prague, Czech Republic, 07 July, 2014, V005T17A019, 10.1115/ ICONE22-30137

[6] Lei, X.; Li, H.; Zhang,W.; Dinh, N. T.; Guo, Y.; Yu, S.: Experimental study on the iffer-ence of heat transfer characteristics between vertical and horizontal flows of supercritical pressure water. Applied Thermal Engineering 113 (2017) 609–620 DOI:10.1016/j.applthermaleng.2016.11.051

[7] Chen, W.; Fang, X.; Xu, Y.; Su, X.: An assessment of correlations of forced convection heat transfer to water at supercritical pressure. Annals of Nuclear Energy 76 (2015) 451–460, DOI:10.1016/j.anucene.2014.10.027

[8] Schatte, G. A.; Kohlhepp, A.; Wieland, C.; Spliethoff, H.: Development of a new empiri-cal correlation for the prediction of the onset of the deterioration of heat transfer to super-critical water in vertical tubes. International Journal of Heat and Mass Transfer 113 (2017) 1333–1341, DOI:10.1016/j.ijheatmasstransfer.2017.04.037

[9] Zhang, Q.; Li, H.; Lei, X.; Zhang, J.; Kong, X.: Study on identification method of heat transfer deterioration of supercritical fluids in vertically heated tubes. International Journal of Heat and Mass Transfer 127 (2018) 674–686, DOI:10.1016/j.ijheatmasstransfer.2018.07.058

[10] Zahlan, H. A. M.; Leung, L. K. H.; Huang, Y.-P.; Liu, G.-X.: Assessment of Convective Heat Transfer Correlations Against an Expanded Database for Different Fluids at Super-critical Pressures. Journal of Nuclear Engineering and Radiation Science 4 (2018) 11004, DOI:10.1115/1.4037720

[11] G.S. Was , P. Ampornrat , G. Gupta , S. Teysseyre , E.A. West , .R. Allen , K. Sridharan , L. Tan , Y. Chen , X. Ren , C. Pister ," Corrosion and stress corrosion cracking in supercritical water" , United States , Journal of Nuclear Materials 371 (2007) 176–201 2007 Elsevier

[12] , Hong Bo Dinh,Jong Min Yu, Kee Bong Yoon, "Thermal Stress Estimation due to Temperature Difference in the Wall Thickness for Thinned Feedwater Heater Tube" *Journal of Energy Engineering*, Vol. 28, No. 3, pp.1~9(2019).

[13] ANSYS Inc (2016). South pointe 2600 ANSYS drive user's guide, 17.2.Canonsburg, PA: ANSYS Inc.